Journal of
Composites Science

MDPI

Article

RF Dielectric Permittivity Sensing of Molecular Spin State Switching Using a Tunnel Diode Oscillator

Ion Soroceanu [1,2], Andrei Diaconu [1,*], Viorela-Gabriela Ciobanu [1], Lionel Salmon [2], Gábor Molnár [2] and Aurelian Rotaru [1,*]

[1] Sci. & Research Center MANSiD, Faculty of Electrical Engineering and Computer, Stefan Cel Mare University, 720 229 Suceava, Romania; ion.soroceanu@usm.ro (I.S.); gabriela.ciobanu@usm.ro (V.-G.C.)
[2] Coordination Chemistry Laboratory (LCC)-CNRS, University of Toulouse, 31077 Toulouse, France; lionel.salmon@lcc-toulouse.fr (L.S.); gabor.molnar@lcc-toulouse.fr (G.M.)
* Correspondence: andrei.diaconu@usm.ro (A.D.); aurelian.rotaru@usm.ro (A.R.)

Abstract: We introduce a novel approach to study the dielectric permittivity of spin crossover (SCO) molecular materials using a radio frequency (RF) resonant tunnel diode oscillator (TDO) circuit. By fabricating a parallel plate capacitor using SCO particles embedded into a polymer matrix as an integral part of the inductor (L) capacitor (C) LC tank of the TDO, we were able to extract the temperature dependence of the dielectric permittivity of frequency measurements for a wide selection of resonance values, spanning from 100 kHz up to 50 MHz, with great precision (less than 2 ppm) and in a broad temperature range. By making use of this simple electronic circuit to explore the frequency and temperature-dependent dielectric permittivity of the compound Fe[$(Htrz)_2$(trz)](BF_4), we demonstrate the reliability and resolution of the technique and show how the results compare with those obtained using complex instrumentation.

Keywords: tunnel diode oscillator; spin crossover; RF dielectric permittivity

Academic Editors: Sambandam Anandan and Francesco Tornabene

Received: 5 November 2024
Revised: 17 December 2024
Accepted: 17 January 2025
Published: 20 January 2025

Citation: Soroceanu, I.; Diaconu, A.; Ciobanu, V.-G.; Salmon, L.; Molnár, G.; Rotaru, A. RF Dielectric Permittivity Sensing of Molecular Spin State Switching Using a Tunnel Diode Oscillator. *J. Compos. Sci.* **2025**, *9*, 49. https://doi.org/10.3390/jcs9010049

1. Introduction

Spin crossover (SCO) materials represent a fascinating class of molecular systems that exhibit reversible transitions between different spin states, typically between a low-spin (LS) and high-spin (HS) configuration. These transitions, driven by external stimuli such as temperature, pressure, light, or electric fields, are of significant scientific interest due to their profound influence on the physical properties of the material [1]. One of the most important aspects of SCO materials is the significant dependence of their electrical properties, such as conductivity and dielectric permittivity, on the spin state [2–4]. The change in spin configuration alters the distribution of electrons within the molecule, affecting the overall electronic structure. As a result, the electrical conductivity can shift considerably when the material switches between its LS and HS states. This spin state-dependent modulation of electrical/dielectric behavior makes SCO materials attractive for applications in smart devices, such as memory storage, sensors, and switches, where the control of electrical properties is crucial [5–7]. Furthermore, the ability to tune these properties through external control adds versatility to their use in next-generation technologies. This unique coupling between spin and electrical properties sets SCO materials apart from other molecular systems and continues to drive research in this area.

We focus our study on the Fe(II) complex [Fe$(Htrz)_2$(trz)](BF_4), one of the most widely studied SCO materials, which can be synthesized from large micro-rods to less than 10 nm

nanoparticles [8,9] and has the advantage of being a robust material with an abrupt transition above room temperature with a large hysteresis width [10].

Here, we propose a novel method to study the RF dielectric properties of SCO materials. Typically used for magnetic susceptibility measurements, the tunnel diode oscillator (TDO) technique uses a simple electronic circuit based on the negative differential resistance of a tunnel diode to sustain oscillations in an LC tank. Since the circuit is always at resonance, minute variations in the values of capacity or inductance of the tank can yield easily measurable changes in frequency. It is a highly sensitive method that allows for the detection of small changes in the permittivity of the insulating material of the capacitor or the permeability of the inductor core. The TDO method is most notably used in low-temperature/high magnetic field physics to investigate the magnetic susceptibility of insulators [11], organic compounds [12], ferromagnetic [13] or superconducting materials [14] as a function of the temperature or applied magnetic field; however, there are very few studies that focus on the dielectric permittivity. In fact, one of the first researchers to perform a comprehensive study of the TDO method, Craig Van Degrift, built an extremely stable TDO circuit (0.001 ppm) to probe the dielectric constant of liquid helium [15].

Our work involves using a SCO-based capacitor as an LC tank component of a TDO circuit to investigate the dielectric permittivity of $[Fe(Htrz)_2(trz)](BF_4)$ particles by measuring induced changes in resonant frequency. We show how this simple technique can be used to study the temperature and frequency dependence of nano-/micro-structured materials in a broad temperature range and for a wide interval of RF frequencies with high resolution.

2. Tunnel Diode Oscillator (TDO) Method

$[Fe(Htrz)_2(trz)](BF_4)$ nanoparticles, synthesized as described in [16], were embedded in a Polyvinylpyrrolidone (PVP) polymer matrix to be used as a dielectric to construct an ITO/SCO+PVP/ITO capacitance assembly. A diagram of the fabrication process is shown in Figure 1. Copper electrodes were attached to the exposed ITO (indium tin oxide) sides of glass slabs using silver paste.

Figure 1. Fabrication process of ITO/SCO+PVP/ITO capacitor.

The obtained capacitor is transparent (Figure 2a), robust and was able to withstand multiple temperature cycles between room temperature (RT) and 155 °C. The active area is ~1 × 0.8 cm^2 with a 25-µm thick SCO+PVP dielectric composite, with a uniform dispersion of SCO nanoparticles in the PVP matrix (Figure 2c). The volume ratio of SCO to PVP in the solid dielectric is 1/10. The capacitance value is around 120 pF. One can easily adapt the capacity to any desired value by modifying the active contact area or dielectric thickness. We also constructed, using a similar approach, a PVP-only capacitor that we tested in

similar conditions to be able to extract, if any, polymer contributions to the dielectric properties results. We chose PVP as the insulating polymer for its availability, transparency and high melting temperature, although we reckon that any similar properties polymer could be used.

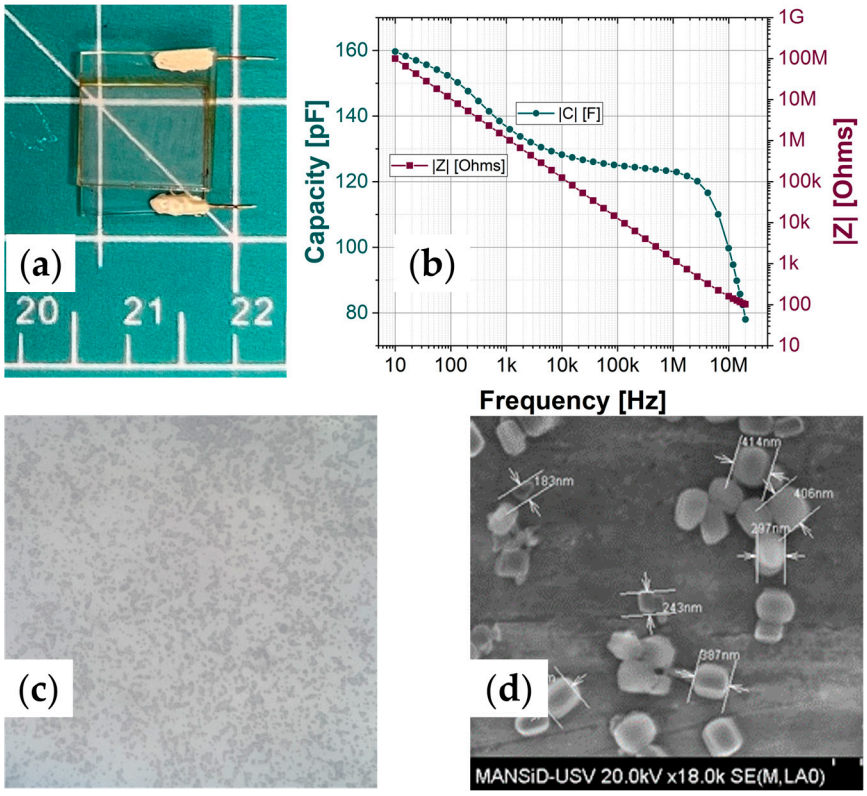

Figure 2. (**a**) ITO/SCO+PVP/ITO dielectric capacitor; (**b**) frequency-dependent capacity and impedance values of the capacitor at RT as measured using broadband dielectric spectroscopy; (**c**) 50× optical image of the SCO+PVP composite film; (**d**) SEM image of Fe[$(Htrz)_2(trz)$](BF_4) particles used.

A major advantage of the method is its simplicity. One only needs a few components and a frequency counter to achieve results comparable with, if not better than, expensive tools. Careful construction of the circuit can yield excellent stability and great resolution. We constructed a circuit to allow us to study the temperature variations in the capacity of our ITO/SCO+PVP/ITO dielectric capacitor by measuring the temperature-induced resonance frequency shift in the TDO.

A scheme of the TDO circuit used is shown in Figure 3. It uses an MBD4057-E28 tunnel diode (Aeroflex/Metelics, Inc., Sunnyvale, CA, USA) along with commercially available components to drive sustained oscillations in an LC tank. The low-power circuit requires a DC source (1–2 V) to operate, a dc-block (or a high-value capacitor), a ×10 amplifier (optional) and a frequency counter. By choosing various values for L and C, we can decide on the resonant frequency. In our setup, we were able to obtain oscillations ranging from 100 kHz to 50 MHz by constructing the LC tank with inductance values ranging from 0.5 µH to 150 µH and capacitor values from 10 pF to 12,000 pF. Our setup has a typical frequency precision of less than 2 ppm at RT, meaning we can detect changes as small as 2 Hz for a 1 MHz resonant frequency, considering that the stability and noise are mostly a result of outside temperature variations and electrical noise.

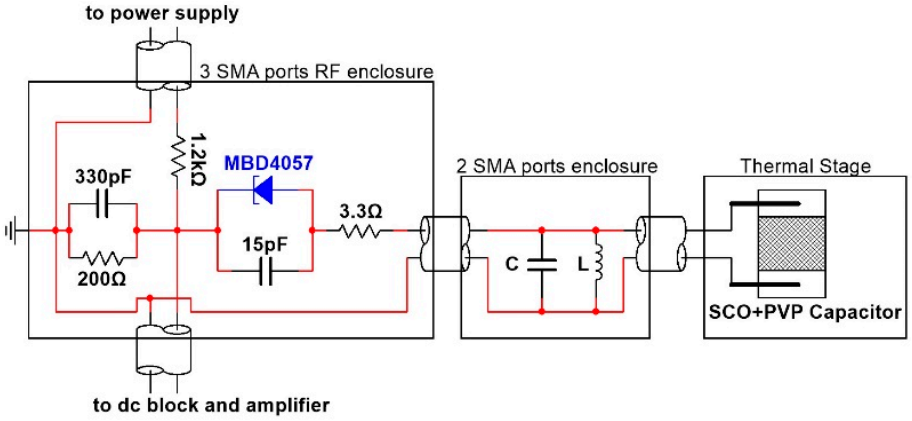

Figure 3. TDO circuit design used for our temperature measurements.

To study the temperature dependence of the SCO+PVP composite, we fitted the capacitor into a liquid nitrogen gas-controlled temperature stage (for thermal uniformity across the capacitor assembly). The capacitor is connected in parallel, via a shielded cable, with the separate LC tank of the TDO circuit, where both the latter are kept at room temperature. A picture of the RT circuit is shown in Figure S1 in the Supporting Information. By choosing various values for L and C, we can choose the frequency of operation and, in turn, the frequency at which we wish to study the SCO-PVP dielectric behavior.

The operational principles of the TDO method are discussed at length in the literature, and in order to have sustained oscillations, some conditions regarding the L and C values must be met [17]. To satisfy the oscillation constraints, we used National Instuments (NI) Multisim^{TM} (Version 14.2.0) software to simulate and select appropriate capacitance and inductance values to achieve the desired frequency. The capacitors used are all NP0 commercial-type capacitors; however, we built the coils in-house. We used COMSOL Multiphysics® (Version 5.2) to simulate the number of magnet wire turns needed to obtain the desired inductance value L and DC resistance values of the coils, which we then built using GE/IMI 7031 Varnish (CMR-Direct, Cambridgeshire, United Kingdom) to encapsulate the solenoid windings. Considering the capacitance value of ~120 pF for our SCO+PVP-based capacitor, we combined various values for the parallel C (namely 0, 470, 1000, 1500 and 10,000 pF) with inductors constructed with different L values (namely 3, 6, 21 and 100 μH) to obtain different resonant frequencies. We were thus able to probe the SCO+PVP dielectric at 7.52 MHz, 4.86 MHz, 2.32 MHz, 1.38 MHz, 873 kHz, 466 kHz and 152 kHz by measuring the frequency variation with temperature.

Since the resonant frequency of the circuit is dependent on most circuit components values, absolute values of L or C are difficult to extract from direct frequency measurements, hence the method is typically used for relative measurements. We are interested in the capacitance, C_T, variation as a function of temperature of our SCO+PVP-based capacitor, which is in a parallel configuration with the fixed capacitance value capacitor in the LC tank (kept at RT). The fixed value C is altered by the parasitic capacitance from connecting cables, which is a function of frequency and insignificantly affected by sweeping temperature variations; we can thus consider it as fixed. Nonetheless, we can achieve absolute capacitance values from the precise estimations of small variations in C_T, as in our case, if we know an approximate initial value. There are more accurate formulas for the resonant frequency of a TDO circuit [17,18], which account for most variables. However, for our measurements, the classical formula is more than adequate. Considering the resonant frequency:

$$f \cong \frac{1}{2\pi\sqrt{L(C + C_T)}} \quad (1)$$

It is easy to show that, for small variations in C_T:

$$\delta C_T = -\frac{\delta f}{2\pi^2 f^3 L} \quad (2)$$

Knowing our L values, we can accurately estimate C_T as a function of temperature as $C_{RT} + \delta C_T$ from frequency measurements, where we consider C_{RT} as the capacity value of the SCO+PVP-based capacitor at RT, as measured by any other capable instrument. The measurement does not have to be very precise, or the value taken at RT. We did, however, consider the RT value of the capacity, as extracted from the data represented in Figure 2b.

All temperature measurements herein were carried out in a similar way and entail three complete heating/cooling thermal cycles between 20 and 130 °C, at a rate of 2 °C/min, with 5 min waiting time at each temperature extrema.

3. Results

The obtained SCO+PVP composite keeps its spin crossover properties, being stable over several successive temperature cycles. Figure 4a shows the temperature dependence of the high spin fraction, n_{HS}, recorded by using a MPMS3 Quantum Design SQUID (Quantum Design, Bucharest, Romania) magnetometer, on a SCO+PVP composite film obtained from drop-casting the same solution used for fabricating our capacitor, albeit with a thicker film for sufficient magnetic signal.

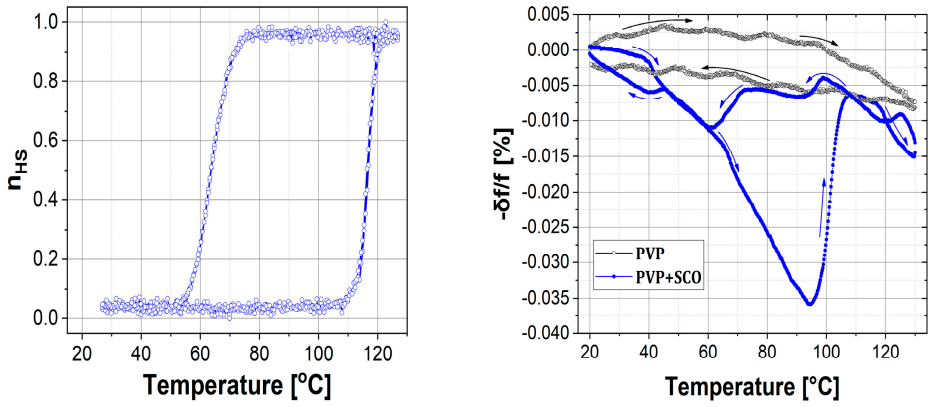

Figure 4. (**a**) High-spin fraction as a function of temperature for the SCO+PVP composite, and (**b**) TDO frequency relative shift as a function of temperature for both the PVP-only and SCO+PVP dielectric capacitors at ~0.9 MHz.

We firstly show one of the data sets obtained from the TDO resonant frequency measurements as a function of temperature for our SCO+PVP-based dielectric capacitor along with the data for the PVP-based capacitor (Figure 4). The curves shown correspond to the second thermal cycles. The first thermal cycle (usually after a period of rest) exhibits strong, subsequently non-repeatable variations in the capacity of both PVP+SCO and PVP-only capacitors, which are most likely due to solvent evaporation or thermal relaxation effects in the PVP polymer (Figure S2).

In this particular case, we used a 21 μH inductor and 1500 pF capacitor for the LC tank with both capacitors. The resonant frequency at RT, i.e., at the start of the second cycle, for the ~120 pF SCP+PVP capacitor is f_{RT} = 872,800 ± 1 Hz, while for the ~80 pF PVP-only capacitor, it is 890,300 ± 1 Hz. The δf values are calculated as the difference in measured frequency f and f_{RT}.

The solid polymer matrix widens the thermal hysteresis of the SCO. Transition temperatures, as extracted from the derivatives extrema of the temperature dependence in

heating/cooling modes, are 113/74 °C for the neat powder and 117/63 °C for the SCO+PVP composite, respectively. In Figure 5, we show the results obtained for the temperature-dependent capacity variations, as estimated using Equation (2), for our SCO+PVP dielectric-based capacitor for seven different resonant frequencies of our TDO circuit.

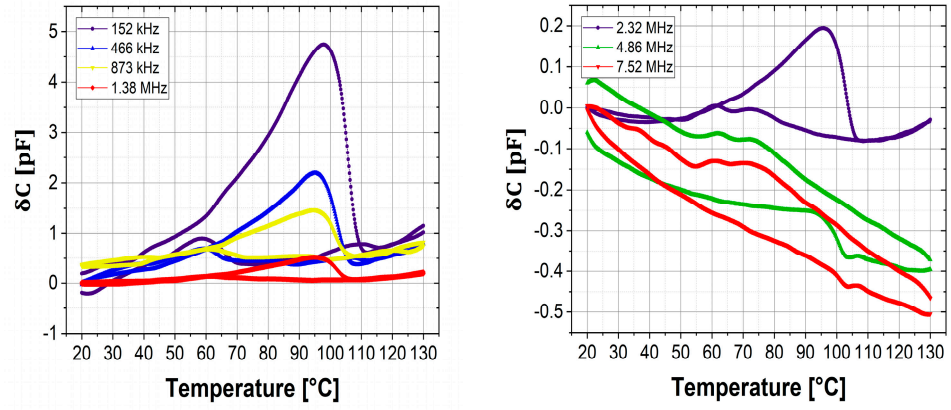

(**a**) (**b**)

Figure 5. Capacity variation with temperature δC_T of $[Fe(Htrz)_2(Trz)](BF_4)$ particles in PVP as extracted from TDO frequency measurements for (**a**) low and (**b**) high frequencies.

The absolute capacity values $C_{RT} + \delta C_T$ can be easily calculated by adding the RT value for a given frequency. For example, at 873 kHz, the room temperature value C_{RT} is 123 pF (see Figure 2b), meaning that the highest LS TDO estimated value is 123 + 1.5 pF. The relative dielectric permittivity can be estimated by knowing the area and separation between the electrodes. The temperature variation of ε_r, as inferred from capacitance results for various TDO frequencies, is shown in Figure 6.

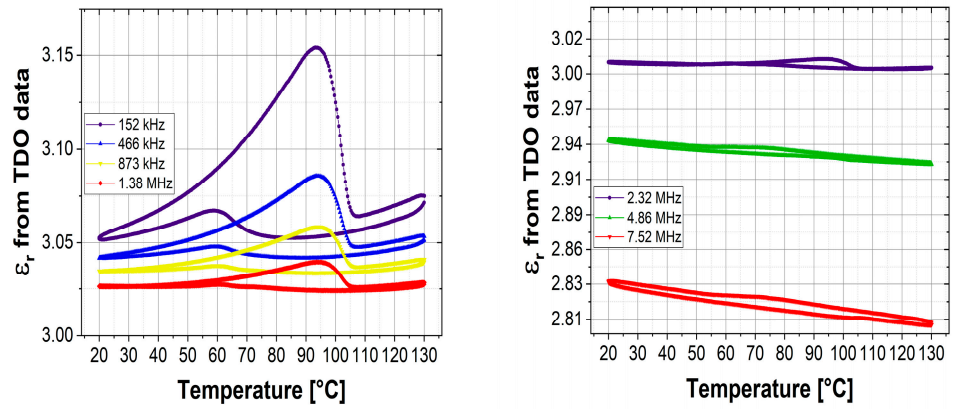

(**a**) (**b**)

Figure 6. Dielectric permittivity of [Fe(Htrz)2(Trz)](BF4) particles in PVP matrix for (**a**) low and (**b**) high frequencies.

If we now plot the frequency dependence of δC_T, which is the capacity value as measured by the TDO minus the capacity value at RT, for several temperatures (Figure 7), we achieve the typical relaxation process of electric dipoles where we have a reduction in dielectric permittivity with increasing frequency [19]. We chose to show δC_T rather than absolute C_T values due to scaling issues in distinguishing any dependence with temperature.

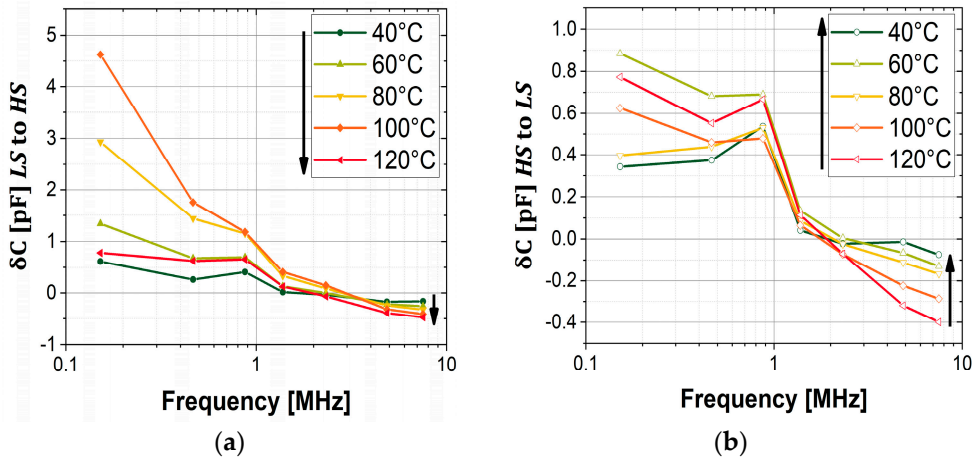

Figure 7. Capacity shift from RT values as a function of TDO resonant frequency for selected temperature values in the (**a**) heating and (**b**) cooling modes.

Figure S3 in the Supporting Information shows the same data, but in absolute values of the TDO capacity. All curves seem to indicate the presence of an inflection point around 600 kHz, with a maximum at ~900 kHz.

4. Conclusions

We show how a tunnel diode oscillator can be used to study the dielectric permittivity of molecular spin crossover particles in variable temperatures and frequencies. The results obtained for $[Fe(Htrz)_2(Trz)](BF_4)$ particles embedded in a PVP matrix, used as dielectric filling for a parallel plate capacitor, show the proof of concept of the TDO method in characterizing the dielectric permittivity of SCO materials. The capacitor can be easily built to accommodate a wide range of materials with various particle shapes and sizes. Due to the micrometric separation of the electrodes, the active dielectric material quantity required is very low. It can be constructed in different shapes, areas and thicknesses, and can be made to resonate with a wide range of inductance and parallel capacity values to allow for a large range of RF excitation frequencies. The construction of the circuit is simple and accessible, with results comparable with complex and expensive instrumentation. One can, in principle, build a TDO circuit to suit a wide range of applications, most notably those that require temperature changes, pressure variations, optical excitation or applied magnetic fields.

Supplementary Materials: The following supporting information can be downloaded at: https://www.mdpi.com/article/10.3390/jcs9010049/s1: Figure S1: The room temperature part of the TDO circuit (containing the LC tank) to be connected in parallel with our SCO+PVP capacitor; Figure S2: Capacity vs. temperature for PVP-only capacitor as measured by dielectric spectroscopy at 900 kHz; Figure S3: Capacity value of the SCO+PVP capacitor as a function of TDO resonant frequency for different temperatures in (a) heating and (b) cooling modes; Figure S4: Raw measurement data using the TDO method vs. impedance spectrometry for 152 kHz and 4.87 MHz.

Author Contributions: Conceptualization, A.D. and A.R.; methodology, A.D. and A.R.; validation, A.D., G.M. and A.R.; formal analysis, I.S., V.-G.C. and L.S.; investigation, I.S., V.-G.C. and L.S.; resources, A.D. and A.R.; data curation, I.S., V.-G.C. and L.S.; writing—original draft, A.D. and A.R.; writing—review and editing, G.M.; supervision, A.D.; funding acquisition, A.D. All authors have read and agreed to the published version of the manuscript.

Funding: This work received funding from UEFISCDI Romania, project number PN-III-P1-1.1-TE-2021-1654 (Contract No: TE 77/2022) and from CNFIS Romania, project number CNFIS-FDI-2023-F-0579.

Data Availability Statement: The data presented in this study is available on request from the corresponding authors.

Acknowledgments: I.S. is grateful for an Eiffel Excellence Scholarship from the French Ministry for Europe and Foreign Affairs.

Conflicts of Interest: The authors declare no conflicts of interest. The funders had no role in the design of the study; in the collection, analyses, or interpretation of data; in the writing of the manuscript; or in the decision to publish the results.

References

1. Halcrow, M.A. *Spin-Crossover Materials: Properties and Applications*; John Wiley & Sons: Hoboken, NJ, USA, 2013.
2. Bousseksou, A.; Molnár, G.; Demont, P.; Menegotto, J. Observation of a Thermal Hysteresis Loop in the Dielectric Constant of Spin-Crossover Complexes: Towards Molecular Memory Materials. *J. Mater. Chem.* **2003**, *13*, 2069–2071. [CrossRef]
3. Lefter, C.; Davesne, V.; Salmon, L.; Molnár, G.; Demont, P.; Rotaru, A.; Bousseksou, A. Charge Transport and Electrical Properties of Spin Crossover Materials: Towards Nanoelectronic and Spintronic Devices. *Magnetochemistry* **2016**, *2*, 18. [CrossRef]
4. Soroceanu, I.; Graur, A.; Coca, E.; Salmon, L.; Molnar, G.; Demont, P.; Bousseksou, A.; Rotaru, A. Broad-Band Dielectric Spectroscopy Reveals Peak Values of Conductivity and Permittivity Switching upon Spin Crossover. *J. Phys. Chem. Lett.* **2019**, *10*, 7391–7396. [CrossRef] [PubMed]
5. Torres-Cavanillas, R.; Gavara-Edo, M.; Coronado, E. Bistable Spin-Crossover Nanoparticles for Molecular Electronics. *Adv. Mater.* **2023**, *36*, 2307718. [CrossRef] [PubMed]
6. Diaconu, A.; Lupu, S.-L.; Rusu, I.; Risca, I.-M.; Salmon, L.; Molnár, G.; Bousseksou, A.; Demont, P.; Rotaru, A. Piezoresistive Effect in the [Fe(Htrz)2(trz)](BF4) Spin Crossover Complex. *J. Phys. Chem. Lett.* **2017**, *8*, 3147–3151. [CrossRef] [PubMed]
7. Kamilya, S.; Dey, B.; Kaushik, K.; Shukla, S.; Mehta, S.; Mondal, A. Realm of Spin State Switching Materials: Toward Realization of Molecular and Nanoscale Devices. *Chem. Mater.* **2024**, *36*, 4889–4915. [CrossRef]
8. Moulet, L.; Daro, N.; Etrillard, C.; Létard, J.-F.; Grosjean, A.; Guionneau, P. Rational Control of Spin-Crossover Particle Sizes: From Nano- to Micro-Rods of $[Fe(Htrz)_2(trz)](BF_4)$. *Magnetochemistry* **2016**, *2*, 10. [CrossRef]
9. Coronado, E.; Galán-Mascarós, J.R.; Monrabal-Capilla, M.; García-Martínez, J.; Pardo-Ibáñez, P. Bistable Spin-Crossover Nanoparticles Showing Magnetic Thermal Hysteresis near Room Temperature. *Adv. Mater.* **2007**, *19*, 1359–1361. [CrossRef]
10. Rotaru, A.; Gural'Skiy, I.A.; Molnár, G.; Salmon, L.; Demont, P.; Bousseksou, A. Spin State Dependence of Electrical Conductivity of Spin Crossover Materials. *Chem. Commun.* **2012**, *48*, 4163–4165. [CrossRef] [PubMed]
11. Habbal, F.; Watson, G.E.; Elliston, P.R. Simple Cryostat for Measuring RF Susceptibility from 4.2 to 300 K. *Rev. Sci. Instrum.* **1975**, *46*, 192–195. [CrossRef]
12. Riet, B.V.; Gerven, L.V. A Cryogenic RE Oscillator, the Heart of a New NMR Dispersion Spectrometer. *J. Phys. E Sci. Instrum.* **1982**, *15*, 558. [CrossRef]
13. Spinu, L.; Srikanth, H.; Gupta, A.; Li, X.W.; Xiao, G. Probing Magnetic Anisotropy Effects in Epitaxial CrO2 Thin Films. *Phys. Rev. B* **2000**, *62*, 8931. [CrossRef]
14. Kim, H.; Tanatar, M.A.; Prozorov, R. Tunnel Diode Resonator for Precision Magnetic Susceptibility Measurements in a mK Temperature Range and Large DC Magnetic Fields. *Rev. Sci. Instrum.* **2018**, *89*, 94704. [CrossRef] [PubMed]
15. Van Degrift, C.T. Tunnel Diode Oscillator for 0.001 ppm Measurements at Low Temperatures. *Rev. Sci. Instrum.* **1975**, *46*, 599–607. [CrossRef]
16. Piedrahita-Bello, M.; Ridier, K.; Mikolasek, M.; Molnár, G.; Nicolazzi, W.; Salmon, L.; Bousseksou, A. Drastic Lattice Softening in Mixed Triazole Ligand Iron(II) Spin Crossover Nanoparticles. *Chem. Commun.* **2019**, *55*, 4769–4772. [CrossRef] [PubMed]
17. Gevorgyan, S.G.; Movsesyan, G.D.; Movsisyan, A.A.; Tatoyan, V.T.; Shirinyan, H.G. Modeling of Tunnel Diode Oscillators and Their use for Some Low Temperature Investigations. *Rev. Sci. Instrum.* **1998**, *69*, 2550–2560. [CrossRef]
18. Van Degrift, C.T.; Love, D.P. Modeling of Tunnel Diode Oscillators. *Rev. Sci. Instrum.* **1981**, *52*, 712–723. [CrossRef]
19. Lefter, C.; Gural'skiy, I.Y.A.; Peng, H.; Molnár, G.; Salmon, L.; Rotaru, A.; Bousseksou, A.; Demont, P. Dielectric and Charge Transport Properties of the Spin Crossover Complex [Fe(Htrz)2(trz)](BF4). *Phys. Status Solidi (RRL)* **2014**, *8*, 191–193. [CrossRef]